

Z-dependence of impurity transport in the Hybrid scenario at JET

C. Giroud¹, P. Belo², R. Barnsley³, I. Coffey³, R. Dux⁴, M. von Hellermann⁵, E. Joffrin⁶, C. Jupen⁷, A. Meigs¹, M. O'Mullane⁸, V. Pericoli Ridolfini⁹, A.C.C. Sips³, A. Whiteford⁸, K-D Zastrow¹ and JET EFDA contributors*.

¹ EURATOM/UKAEA Fusion association, Culham Science Centre, Abingdon OX14 3DB, U.K.

² EURATOM/IST Fusion Association, Centro de Fusão Nuclear, 1049-001 Lisbon Portugal

³ Department of Physics, Queens University, Belfast, U.K.

⁴ Max Planck Institut Plasmaphysik, EURATOM Association, Garching, Germany.

⁵ FOM-Instituut voor Plasmafysica 'Rijnhuizen', Associatie Euratom-FOM, Trilateral Euregio Cluster, P.O. Box 1207, 3430 BE Nieuwegein, the Netherlands.

⁶ Association EURATOM-CEA, CEA Cadarache, F13108 St. Paul lez Durance, France.

⁷ Department of Physics, University of Lund, Sölvegatan 14, 223 62 Lund, Sweden

⁸ Department of Physics and Applied Physics, University of Strathclyde, Glasgow, U.K.

⁹ Associazione EURATOM-ENEA sulla Fusione, Frascati, 00044 Italy.

*Annex J. Pamela et al, Fusion Energy 2002. Proc 19th IAEA Fus. Energy Conf., Lyon 2002.

1. Introduction

Impurity transport is an important issue for the development of ITER scenarios. Indeed, impurity accumulation can lead to severe radiated power loss (from high Z impurities not fully ionised in the core), fuel dilution (for both low and high Z impurities) and can affect plasma stability. All of these issues need to be dealt with to achieve steady state operation. It is therefore important to gather knowledge on the Z-dependence of impurity transport in the ITER relevant scenarios. A new method to study the Z-dependence of impurity transport has been developed and is presented in this paper. This method allowed us to characterise impurity transport in the Hybrid scenario at JET.

2. Experimental technique

A new technique has been developed to minimise errors in the deduced Z dependence of impurity transport. This technique consists of injecting simultaneously Ne and Ar with the same edge gas fuelling valve. The choice of Ne and Ar was motivated by the vicinity of their charge-exchange lines (NeX 5249Å, ArXVIII 5224 Å) to the routinely measured CVI spectra (5290Å). The ArXVIII, NeX and CVI densities are thus locally measured at the same time, spatial position and on the same spectrometer thus avoiding any systematic error. It was determined experimentally that a gas mix of 70% Ar and 30% Ne allows sufficient photon flux for both ArXVIII and NeX charge-exchange lines while minimising the amount

of impurity introduced. On the hybrid scenario discharge, one Ar/Ne puff of a 100ms was sufficient to determine the impurity transport and only introduced about 7×10^{18} Ne atoms and 2×10^{19} Ar atoms. The Ar/Ne injection on the plasma discharge introduce a rise of Z_{eff} of 20%, as can be seen in figure 1, and increased dilution of 1.5% and 1.8% for Ne and Ar. Such moderate impact on the plasma discharges allows this method to be used parasitically to probe many discharges during the 2003-2004 JET campaigns.

3. Transport model and fitting technique

The Ar and Ne transport is monitored by three spectroscopic diagnostics: charge-exchange, Vacuum Ultra-Violet (VUV) and X-ray grazing incidence spectrometers. The VUV and X-ray spectrometers are absolutely calibrated and measure line-of-sight integrated absolute intensities of Ar¹⁴⁺ 221 Å, Ar¹⁵⁺ 353.9 Å, Ar¹⁶⁺ 3.94 Å, Ar¹⁷⁺ 3.73 Å, Ne⁷⁺ 770-780 Å and Ne⁹⁺ 10.24 Å. The Ar¹⁸⁺ and Ne¹⁰⁺ densities profiles are measured with the charge-exchange diagnostic. The Ar impurity transport coefficients, diffusion D and convection V, are deduced from a least-square fit of the modelled Ar¹⁸⁺ densities and Ar¹⁵⁺ line intensities with a $1^{1/2}D$ transport model code (UTC SANCO). In the case of Ne, the fit was performed with Ne¹⁰⁺ densities and Ne⁷⁺ line intensity (when not too noisy). The transport coefficients D, diffusion, and V, convection, were kept constant in time. The initial influx corresponding to Ar/Ne puff has been modelled. It is assumed that a factor R of the particles leaving the LCFS is reintroduced as influx.

As seen in figures 2 and 3 for the hybrid discharge #60932, the model reproduces both CXRS data and absolute intensities of VUV lines which validates our description of the transport both in the core and edge regions. Added to that, the X-ray measurements for Ar, not used in the fit, were also well reproduced in time dependence and absolute terms. However, the X-ray measurements for Ne were badly reproduced as the modelled intensities were about a factor 10 below the measurements, which points out to a calibration problem. It remains to be investigated why the modelled Ar¹⁴⁺ is too high by ~ 2 in absolute values. However, the modelled time dependence of Ar¹⁴⁺ compared well with experiments.

4- Hybrid scenarios and Results

The hybrid scenario is one of the scenarios envisaged for ITER [1][2]. It is an intermediate scenario between the baseline ELMy H-mode, relying on inductive current drive operation, and advanced scenarios, relying on non-inductive current drive operation. The hybrid

scenario has an increased non-inductive current fraction (from baseline ELMy H-mode) together with increased stability. This scenario has been documented at JET for different dimensionless parameter variations, such as with ρ^* at constant q_{95} and with triangularity [1].

The transport coefficients, i.e. D and V , of Ar and Ne have been determined for five hybrid discharges with different ρ^* at constant q_{95} ($4.4\text{-}5.8 \times 10^{-3}$) and two triangularities ($\delta=0.2$ and $\delta=0.44$), see Table 1. As can be seen in figure 5, the Ar and Ne convection for the hybrid discharge can be divided into three regions of transport: a central region from $r/a \sim 0\text{-}0.3$ with low convection, a middle region from $0.3\text{-}0.7$ with a negative convection and finally an edge region from $r/a \sim 0.7\text{-}1$. Ar and Ne convection show the same features however the magnitude is usually lower for Ne by a factor 2-3 at $r/a \sim 0.4$ and $r/a \sim 0.8$. A comparison with the neoclassical coefficients determined from JETTO-NCLASS, plotted in figure 5, show that the diffusion is clearly strongly anomalous both for Ar and Ne. The Ar and Ne convection is anomalous but close to neoclassical values at the edge.

The change of ρ^* at constant q_{95} has similar consequences for both Ar and Ne. Figure 6 shows the example of Ar but the conclusion holds for Ne. It can be seen that the diffusion decreases by a factor ~ 2 at high triangularity, whereas no real change is seen for low triangularity. The convection, on the other hand, remains approximatively constant when decreasing ρ^* at constant q_{95} for both low and high triangularity.

The effect of a change of triangularity has also been studied. As the triangularity increases from $\delta=0.2$ to $\delta=0.44$, the convection in the edge region changes from outward to inward. This effect has also been observed for high ρ^* case. This could be explained neoclassically by a change of gradient between density and temperature, but remains to be tested. It is also important to observe that the Ar and Ne diffusion is reduced by a factor 2 in the edge region with an increase of triangularity.

4. Conclusion

A new technique for the study of Z-dependence of impurity transport has been developed and its potential to be used parasitically to the main discharge has been proven. This technique has been applied to hybrid scenarios. Both Ne and Ar transport models were successful in reproducing both edge and core measurements in absolute values. In hybrid scenarios, both diffusion and convection are anomalous, although the convection can be

close to the neoclassical values at the edge. More importantly, a change from outward to inward convection has been shown when increasing triangularity for both low and high ρ^* . Work performed under the European Fusion Development Agreement and partly funded by Euratom and the UK Engineering and Physical Sciences Research Council. [1] A.C.C sips et al EPS 2003 [2] C. Gormezzano this conference

← scan in ρ^* at q_{95} const

scan in triangularity δ $\delta=0.44$ $\delta=0.2$	#60931 $\rho^*=0.058$ $B_T=1.7\text{ T}, I_p=1.4\text{ MA}$	#62490 $\rho^*=0.044$ $B_T=2.4\text{ T}, I_p=2\text{ MA}$
	#60926 $\rho^*=0.066$ $B_T=1.7\text{ T}, I_p=1.4\text{ MA}$	#60933 #60932 $\rho^*=0.055$ $B_T=2.4\text{ T}, I_p=2\text{ MA}$

Table 1: Discharges analysed in the hybrid discharges study

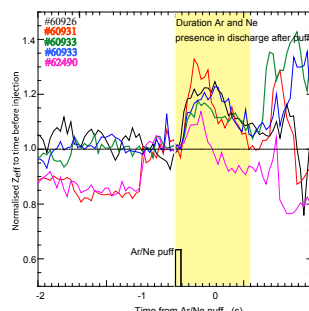


Figure 1: Increase of line average Z_{eff} due to Ar/Ne puff: on the hybrid scenario, the increase in Z_{eff} is ~20%.

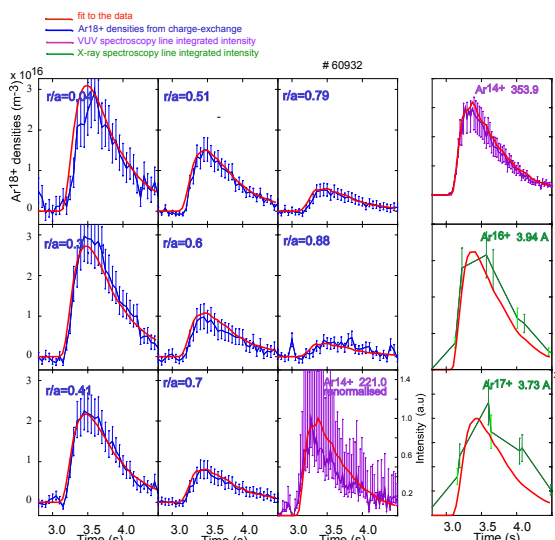


Figure 2: Argon modelled densities and line intensities against CXRS, VUV and X-ray measurements.

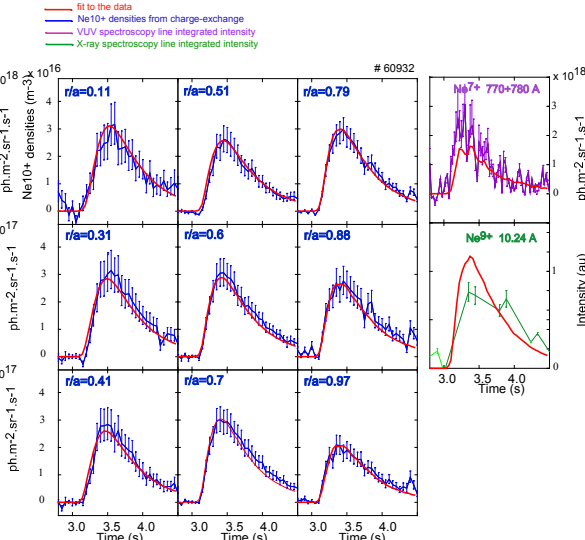


Figure 3: Neon modelled densities and line intensities against CXRS, VUV and X-ray measurements.

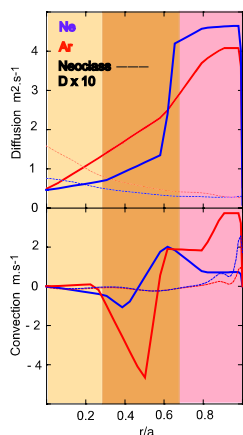


Figure 5: Comparison between Ar and Ne transport coefficient for hybrid scenarios: three regions with different transport can be seen in the convection. The neoclassical values are shown in dashed lines.

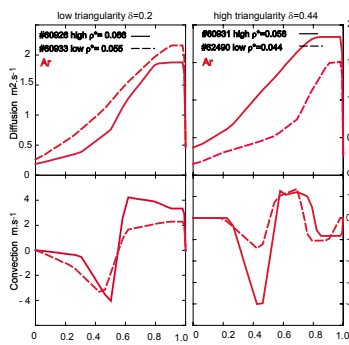


Figure 6: D and V dependence with ρ^* at constant q_{95} : Argon transport coefficients are plotted for each triangularity for low and high ρ^* .

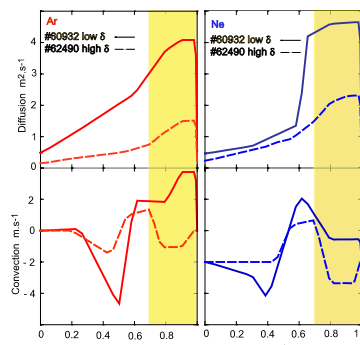


Figure 7: V and D dependence on triangularity: A change from outward to inward convection is seen in the edge region for both Ne and Ar.